Transient Focal Membrane Deformation Induced by Arginine-rich Peptides Leads to Their Direct Penetration into Cells

Hisaaki Hirose[1], Toshihide Takeuchi[1,5], Hiroko Osakada[2], Sílvia Pujals[1], Sayaka Katayama[1], Ikuhiko Nakase[1], Shouhei Kobayashi[2], Tokuko Haraguchi[2–4] and Shiroh Futaki[1]

[1]Institute for Chemical Research, Kyoto University, Kyoto, Japan; [2]Advanced ICT Research Institute Kobe, National Institute of Information and Communications Technology, Hyogo, Japan; [3]Graduate School of Frontier Biosciences, Osaka University, Osaka, Japan; [4]Graduate School of Science, Osaka University, Osaka, Japan; [5]Present address: National Institute of Neuroscience, National Center of Neurology and Psychiatry, Tokyo, Japan

Endocytosis has been implicated in the cellular uptake of arginine-rich, cell-penetrating peptides (CPPs). However, accumulating evidence suggests that certain conditions allow the direct, non-endocytic penetration of arginine-rich peptides through the plasma membrane. We previously showed that Alexa Fluor 488-labeled dodeca-arginine (R12-Alexa488) directly enters cells at specific sites on the plasma membrane and subsequently diffuses throughout cells. In this study, we found that the peptide influx was accompanied by the formation of unique, "particle-like" multivesicular structures on the plasma membrane, together with topical inversion of the plasma membrane. Importantly, the conjugation of dodeca-arginine (R12) to Alexa Fluor 488 or a peptide tag derived from hemagglutinin (HAtag) significantly accelerated particle formation, suggesting that the chemical properties of the attached molecules (cargo molecules) may contribute to translocation of the R12 peptide. Coincubation with R12-HAtag allowed the membrane-impermeable R4-Alexa488 to permeate cells. These results suggest that R12 peptides attached to hydrophobic cargo molecules stimulate dynamic morphological alterations in the plasma membrane, and that these structural changes allow the peptides to permeate the plasma membrane. These findings may provide a novel mode of cell permeabilization by arginine-rich peptides as a means of drug delivery.

Received 7 September 2011; accepted 26 December 2011; advance online publication 14 February 2012. doi:10.1038/mt.2011.313

INTRODUCTION

Intracellular delivery using cell-penetrating peptides (CPPs; also known as protein transduction domains) has received major attention as a novel method of efficiently introducing exogenous molecules into cells.[1,2] Among them, arginine-rich peptides including oligoarginine and HIV-1 Tat (48–60) are regarded as one of the representative classes of CPPs that facilitates efficient translocation through biological membranes.[3–8] However, the detailed membrane translocation mechanisms of these peptides are still being debated. Recent studies using intact living cells showed endocytic pathways including macropinocytosis to be major routes for internalization of these peptides.[9–14] However, accumulating evidence indicates that the internalization mechanisms of arginine-rich peptides differ according to the administration conditions (e.g., peptide sequence, peptide concentration, cell type, and culture medium) and that endocytosis may not be the sole mechanism of internalization of arginine-rich peptides.[14–16] Studies by us and others on cellular localization using fluorescently labeled arginine-rich peptides have shown that octa-arginine (R8) and Tat peptides yield diffuse signals when applied to cells at a temperature of 4 °C in the presence of endocytosis inhibitors including 5-(*N*-ethyl-*N*-isopropyl)amiloride (EIPA) and methyl-β-cyclodextrin, while maintaining membrane integrity.[15,16] The endocytic uptake of these peptides would yield endosome-like punctate signals in the cytoplasm. The diffuse signals from the internalized peptides under endocytosis-suppressing conditions are instead highly suggestive of the presence of direct translocation pathways.

More recently, we conducted a detailed study on the relationship between administered concentration and eventual cellular localization of dodeca-arginine (R12), a peptide that should interact more strongly with cell surface molecules than R8 or Tat.[16] At relatively low concentrations, R12 labels endosome-like structures, yielding punctate signals similar to those for R8 and Tat peptides. When the peptide concentration exceeds a certain threshold, however, diffuse cytosolic labeling for R12 was predominantly observed, which was accompanied by a dramatic increase in overall cellular fluorescence. The mechanism involved cannot be simple passive diffusion through the lipid bilayer because the diffusion is only initiated at specific sites on the plasma membranes.[16]

In the present study, using an Alexa Fluor 488-labeled R12 peptide (R12-Alexa488), whose Alexa Fluor 488 moiety (molecular weight ~700) can be regarded as a model of low-molecular-weight cargo molecules, we showed that interaction with the peptide caused dynamic structural alterations in the plasma membrane and induced the formation of unique "particle-like" structures composed of multiple vesicles on the plasma membrane,

The first two authors equally contributed to this work.

Correspondence: *Shiroh Futaki, Institute for Chemical Research, Kyoto University, Uji, Kyoto 611-0011, Japan. E-mail: futaki@scl.kyoto-u.ac.jp*

together with direct influx of the peptide into the cytosol. We also showed that attachment of the fluorescent moiety or a peptide tag derived from positions 98–106 of human influenza hemagglutinin (HAtag, YPYDVPDYA) significantly stimulated particle formation, suggesting that direct penetration of R12 is greatly accelerated by the attachment of hydrophobic cargo molecules. Moreover, an Alexa Fluor 488-labeled R4 peptide (R4-Alexa488) and Alexa Fluor 488-labeled Gly-Cys-amide (GC-Alexa488), which usually show very little internalization, translocated through the plasma membrane into the cytosol when coincubated with R12-HAtag, while causing no major cytotoxicity to the cells.

RESULTS

Time-lapse imaging of direct internalization of the R12-Alexa488 peptide into cells

The direct translocation of R12-Alexa488 into living HeLa cells, and subsequent distribution, were analyzed by confocal microscopy. The final concentration of R12-Alexa488 in the medium was 5 µmol/l, which corresponds to the threshold value in serum-free medium for accomplishing direct translocation into the cytosol.[16] The fluorescent signal for R12-Alexa488 was detected in the cytosol as early as a few minutes after the addition of the peptide to the culture medium, and was typically detected in more than 80% of cells within 15 minutes (**Figure 1a**, upper panels). Entry of the peptide into the cytosol was initiated at specific sites with strong fluorescent signals and then spread throughout the entire plasma membrane (arrows in **Figure 1a**; see also **Supplementary Figure S1** and **Supplementary Video S1**), as previously reported by us and others.[14–16]

Simultaneous observation of the peptide-treated cells by differential interference contrast microscopy revealed that the direct internalization of R12-Alexa488 was accompanied by the formation of small particle-like structures ~1–3 µm in diameter on the plasma membrane (see lower panels of **Figure 1a**; compare with the lower and upper panels (arrows) in **Figure 1a**). Note that the locations of these particles on the plasma membrane exactly coincided with the points of peptide influx (**Figure 1a**, upper panels). The topology of the particle structures was further analyzed by staining the cell membranes with the nonspecific membrane dye FM4-64 (see **Supplementary Figure S2**). Z-stack analysis of the particles showed excellent three-dimensional agreement with the R12-Alexa488 signals, suggesting the involvement of both membrane components and R12-Alexa488 in the formation of these particles. The influx of R12-Alexa488 at these specific sites was transient, with a typical duration of 10–20 minutes. The particles gradually became larger in size in response to influx of the peptide into cells (arrows in **Figure 1a**) and often retained their structure even after no further peptide influx was observed. Multiple sites of influx in individual cells were often formed in turn during treatment with R12-Alexa488 (as indicated by the arrows at 4 minutes in **Figure 1a**). In contrast, R4-Alexa488, which has only poor translocation ability, had no significant effect on the cellular membranes, even when applied at a threefold higher concentration (**Supplementary Figure S3b**), suggesting that the number of arginine residues may be a critical factor in the influx of peptides into cells.

Note that the influx sites for R12-Alexa488 were always accompanied by particulate membrane structures. Moreover, peptide influx and particle structure formation also occurred at low temperatures (4 °C and 15 °C) (**Figure 1b** and **Supplementary Figure S3a**), suggesting that these processes are energy-independent and thus probably do not require active transport machineries.[15] The energy independence of particle formation was further confirmed by assessing particle formation in the presence of macropinocytosis inhibitors. Macropinocytosis has been reported to be one of the major pathways for the internalization of arginine-rich peptides.[10] Treatment of cells with the representative macropinocytosis inhibitors EIPA and cytochalasin D (CytD) did not affect the induction of membrane particle formation by R12-Alexa488 (**Supplementary Figure S4**). Also, in the presence of EIPA, enhanced cytosolic penetration of the peptide through the plasma membrane was observed, consistent with the results of a previous study in which fluorescein-labeled R9 and Tat were used.[14] Many more membrane particles were formed in the presence of EIPA compared to control conditions, in accord with the enhanced influx of R12-Alexa488 into cells (**Supplementary Figure S4**). The above results further suggest that the diffusion of R12-Alexa488 into HeLa cells accompanying membrane particle

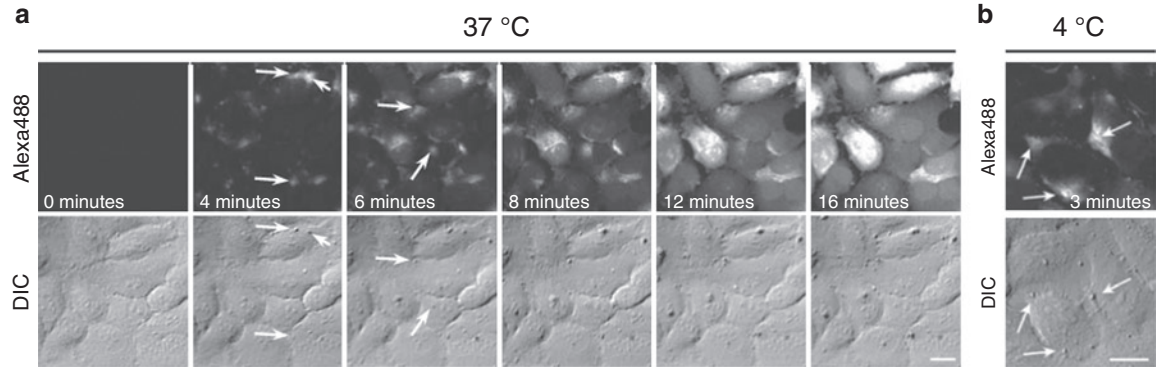

Figure 1 Direct internalization of R12-Alexa488 into the cytosol accompanied by the formation of particle-like structures on the plasma membrane. (**a**,**b**) Time-lapse images of cells incubated with R12-Alexa488 (5 µmol/l) in serum-free medium (α-MEM(–)) at (**a**) 37 °C and (**b**) 4 °C. Upper panels (labeled "Alexa488") show time-lapse fluorescence images for Alexa Fluor 488. Lower panels (labeled "DIC") present differential interference contrast (DIC) images of the same fields shown in the upper panels. Arrows indicate peptide influx points (fluorescence images for Alexa Fluor 488) and membrane particles (DIC images). Time 0: images captured immediately before the addition of R12-Alexa488. Bar = 20 µm. MEM, minimum essential medium.

formation is independent of energy-dependent cellular machineries, including macropinocytosis.

Membrane potential was previously reported to play a critical role in the internalization of arginine-rich peptides into cells.[7] We therefore examined whether particle formation was dependent on the membrane potential. Under physiological conditions, high Na^+ levels in the extracellular environment and high K^+ levels in the cytosol maintain a transmembrane potential. Replacement of Na^+ in the extracellular fluid with K^+ diminishes this transmembrane potential. We thus employed a K^+-rich buffer (K^+ concentration 140 mmol/l) as the extracellular medium (**Supplementary Figure S5a**).[17] When HeLa cells were incubated with R12-Alexa488 (5 µmol/l) in Na^+-rich buffer (Na^+ concentration 140 mmol/l), which maintained the normal membrane potential, membrane particles were formed as described above (**Supplementary Figure S5a**, upper panels). In contrast, significant particle formation and R12-Alexa488 influx into cells were not observed using the K^+-rich buffer (**Supplementary Figure S5a**, lower panels). Even when R12-Alexa488 was applied at a concentration of 20 µmol/l, no significant membrane particle formation was detected in the K^+-rich buffer (data not shown). These results suggest that membrane particle formation is affected by K^+ ion concentration, or the membrane potential. This was further confirmed by the recovery of R12-Alexa488 influx into cells and membrane particle formation when an excess of the Na^+-rich buffer was applied to cells that had initially been treated with the K^+-rich buffer (see **Supplementary Figure S5b**). These results strongly suggest that interaction of the peptide with cell surfaces is not sufficient for the formation of membrane particles, and that a membrane potential is required for the influx of R12-Alexa488 into cells via the plasma membrane.

Plasma membrane inversion accompanies R12 internalization

The influx of R12-Alexa488 through the plasma membrane may be accompanied by migration of the membrane and associated molecules, thereby leading to membrane inversion. Phosphatidylserine is a membrane component that under normal conditions is primarily localized to the inner side of the plasma membrane. Plasma membrane disorder, such as that induced by apoptosis, can lead to inversion of the membrane, and thus the presentation of phosphatidylserine at the cell surface. This can be detected with a specific binding partner, the protein annexin V.[11]

Significant signals for Alexa Fluor 568-labeled annexin V were detected in HeLa cells that had been coincubated with the R12-Alexa488 (**Figure 2a**). In addition, these annexin V signals were highly colocalized with both the sites of peptide influx and the particles that transiently formed on the membranes (**Figure 2a**, arrows). In contrast, no significant annexin V signals were detected in cells treated with the R4-Alexa488 (**Figure 2b**). These observations provide direct evidence that peptide treatment induces the dynamic movement of membrane molecules, accompanied by membrane inversion, in the extremely limited regions corresponding to the peptide influx sites. Note that although several phosphatidylserine signals in the outer cellular membrane were detected by annexin V staining, no apoptotic cell death was observed in cells treated with R12 under the described conditions (data not shown).

Accumulation of membrane-associated molecules to the sites of R12-Alexa488 internalization

The above results strongly suggest that the direct influx of R12-Alexa488 may be accompanied by the dynamic rearrangement of other membrane-associated molecules. Acidic membrane-associated molecules could realistically be expected to interact with the basic R12. We therefore monitored the dynamic behavior of the ganglioside GM1 following R12-Alexa488 treatment using Alexa Fluor 555-labeled cholera toxin subunit B (CTxB-Alexa555), a reagent that specifically binds to GM1,[18] a representative sialic glycolipid with one sialic acid moiety in its terminus. Strong CTxB signals were detected at sites of the peptide influx, and thus particle formation, in cells treated with R12-Alexa488 (**Figure 3a**). In contrast, no such signals were detected in cells treated with R4-Alexa488 (**Figure 3b**), suggesting that GM1 may interact with R12.

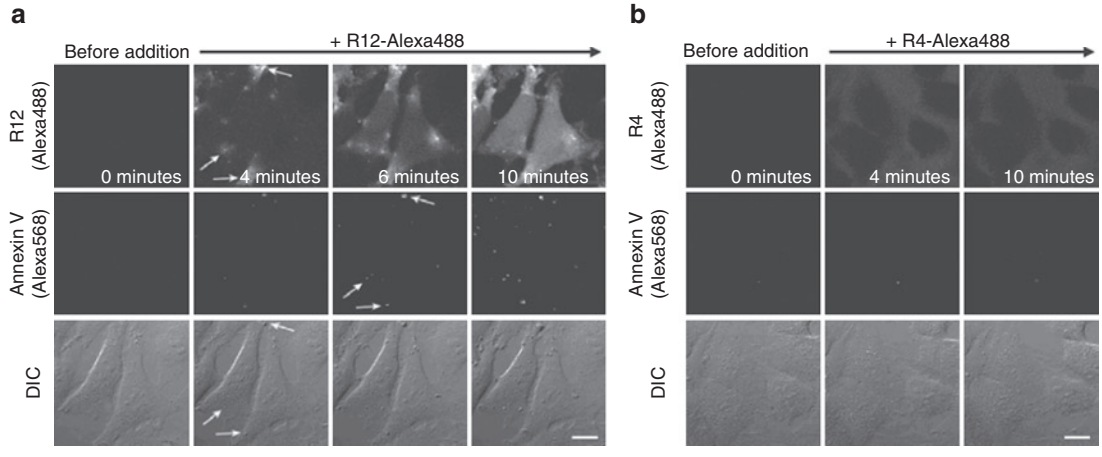

Figure 2 Membrane inversion coupled with influx of R12-Alexa488 into the cytosol. Time-lapse images of cells incubated with (**a**) R12-Alexa488 (5 µmol/l) or (**b**) R4-Alexa488 (15 µmol/l) in α-MEM(–) at 37 °C in the presence of annexin V-Alexa568. Upper, middle, and lower panels show fluorescent images of R12-Alexa488, fluorescent images of annexin V-Alexa568, and DIC images in the same fields, respectively. Arrows in **a** indicate sites of peptide influx (upper panel), annexin V signals (middle panel), and membrane particles (lower panel), respectively. Time 0: images captured immediately before the addition of the arginine peptides. Bar = 20 µm. DIC, differential interference contrast; MEM, minimum essential medium.

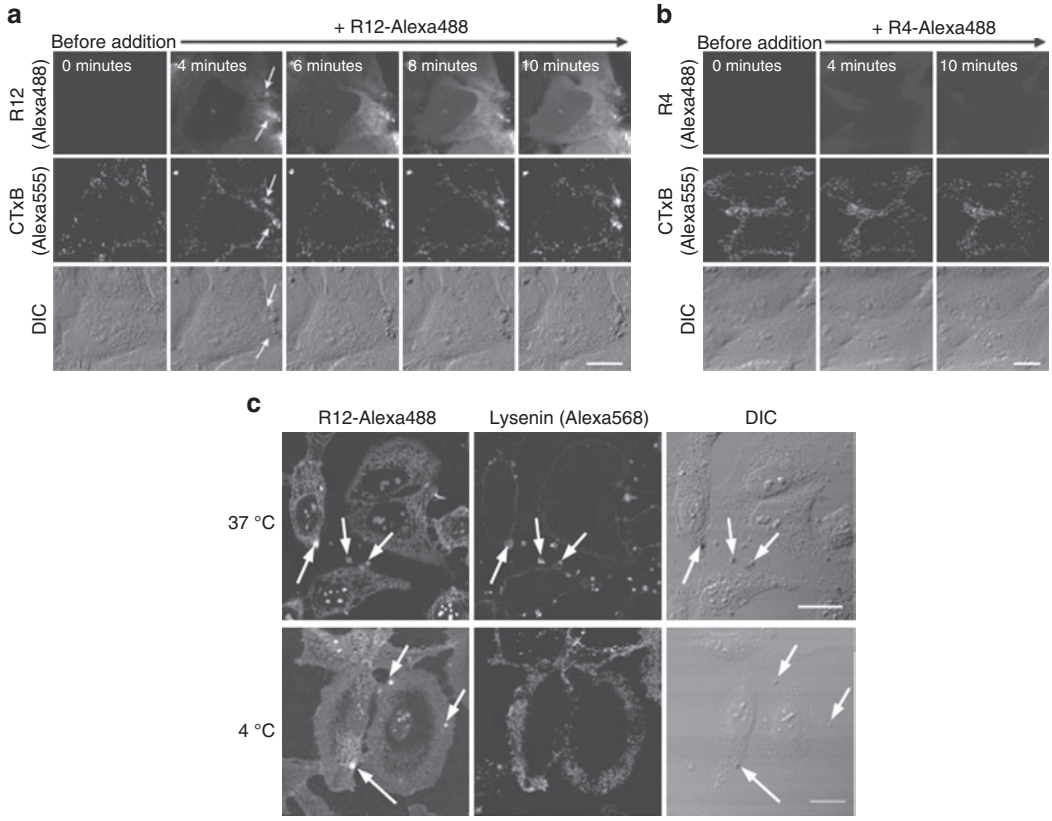

Figure 3 Recruitment of GM1 and sphingomyelin to the sites of peptide internalization. (**a**,**b**) Time-lapse images of cells incubated with 5 µmol/l (**a**) R12-Alexa488 or (**b**) R4-Alexa488 in serum-free medium (α-MEM(–)) at 37 °C. The arrows in **a** indicate sites of cholera toxin subunit B (CTxB) signals, peptide influx (R12), and membrane particle formation (DIC). Time 0: images captured immediately before the addition of the arginine peptides. (**c**) Immunofluorescence staining with lysenin, a sphingomyelin-specific probe. The localization of lysenin in HeLa cells incubated with R12-Alexa488 (5 µmol/l) for 5 minutes at 37 °C or 4 °C is shown. Arrows indicate sites of membrane particles. Bar = 20 µm. DIC, differential interference contrast.

Since sialic glycolipids have been suggested to be abundant in lipid raft microdomains,[18] we studied the possible involvement of lipid raft microdomains in particle formation. Lipid raft microdomains have been reported to be rich in cholesterol and sphingomyelin (SM).[19] We used the SM-specific probe lysenin[20] to monitor the localization of SM in cells incubated with R12-Alexa488 (**Figure 3c**). Treatment of cells with R12-Alexa488 led to significant SM accumulation at the sites of membrane particles (compare the three horizontal panels (arrows) in **Figure 3c**), suggesting a role for microdomains in particle formation. However, the formation of membrane particles and accumulation of SM were also observed when cells were also treated with MβCD, a reagent that extracts cholesterol from cell membranes and thereby disrupts lipid raft/caveolae microdomains (**Supplementary Figure S6**). This suggests that lipid raft/caveolae microdomains may not be indispensable for particle formation.

Membrane particles were formed at 4 °C, but SM did not accumulate at the sites of particle formation at this temperature (**Figure 3c**). This indicates that the lipid composition of the membrane particles may be different at 4 °C and 37 °C, perhaps because of a decrease in the lateral diffusion of membrane lipids at 4 °C. Therefore, the mechanisms by which the particles are formed at 4 °C and 37 °C may not be identical.

Structural analysis of membrane particles by electron microscopy

To obtain more information about the detailed structures of the membrane particles formed following peptide treatment, electron microscopic analysis was conducted. For electron microscopy, fixation procedure of samples with, for example, 2% glutaraldehyde, is usually necessary before osmium tetroxide treatment and dehydration. However, artifacts in the cellular localization of arginine-rich peptides caused by fixation have been noted.[9] Therefore, we carefully reassessed the effects of fixation on the cellular localization and on internalization of the R12 peptide using acetone/methanol (1:1), 4% paraformaldehyde (PFA), and 2% glutaraldehyde (GA) as fixation reagents (**Supplementary Figure S7**). We found no significant artifacts in the cellular localization of R12-Alexa488 when using either 4% paraformaldehyde or 2% GA, as long as we avoided using mounting media for microscopic observation. When we used 2% GA under conditions allowing both endocytic uptake and direct diffusion into the cytosol, signals for R12-Alexa488 were particularly well retained, even after fixation (**Supplementary Figure S7**). Two percent GA in 30 mmol/l 4-(2-hydroxyethyl)-1-piperazineethanesulfonic acid (HEPES) is a standard solution for primary fixation when performing electron microscopic analysis. We thus obtained electron micrographs of cells treated

with R12-Alexa488 after 2% GA fixation followed by osmium tetroxide treatment and dehydration (**Figure 4**).

Detailed structures of the membrane particles formed after treatment with R12-Alexa488 were clearly observed by scanning electron microscopy. Unexpectedly, the magnified images of these particles revealed that they did not have a simple large vesicular structure, but instead consisted of many small vesicles of various diameters (~50–500 nm) (**Figure 4a**). In addition, smaller, presumably "immature" particles consisting of one or a few vesicles were observed throughout the membranes of peptide-treated cells, whereas no such vesicles were detected in control cells (**Figure 4b**). This suggests that treatment with R12-Alexa488 induces the formation of these vesicles on plasma membranes and that their eventual accumulation results in formation of the large particles identified by confocal microscopy as the sites of peptide influx. The vesicle-stacking structures of these particles were further studied by transmission electron microscopy (TEM). Analysis of vertical sections of peptide-treated cells revealed the complex structures of the particles (**Figure 4c**). The vesicles from which the membrane particles were formed consisted of multilamellar lipid membranes, each with an internal hollow space (**Figure 4c**). Significant formation of particle structures was not observed in the cells that were not treated with the peptide (**Figure 4d**).

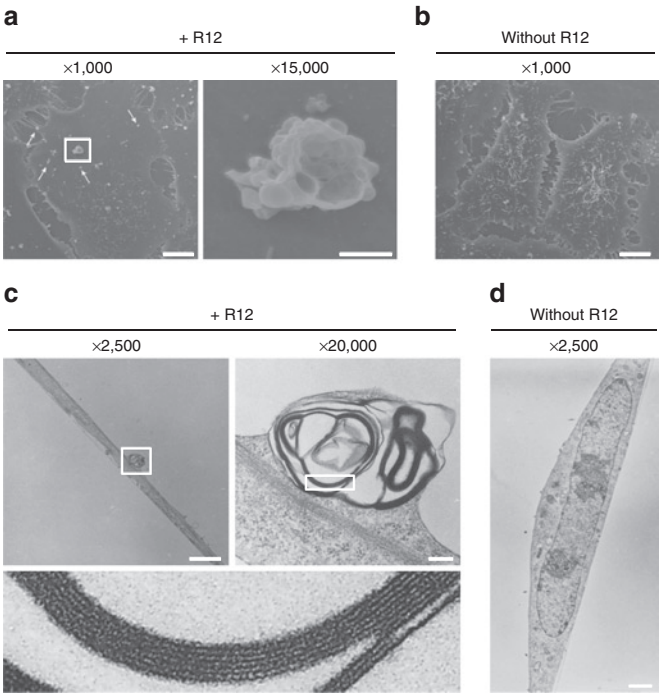

Figure 4 Electron microscopic analysis showing that the membrane particles formed following R12-Alexa488 treatment consist of multiple multilamellar vesicles stacked on top of each other. (**a**,**b**) HeLa cells were treated (**a**) with or (**b**) without R12-Alexa488 (6 µmol/l) in α-MEM(–) for 5 minutes, fixed through incubation with 2% glutaraldehyde in 30 mmol/l HEPES, and then analyzed by SEM. The right image in **a** is a magnified image of the membrane particle highlighted in the left image. Arrows indicate single vesicles or immature particles composed of small numbers of vesicles. (**c**,**d**) Cells were treated (**c**) with or (**d**) without R12-Alexa488 as in **a**,**b** and analyzed by TEM. The upper-right image in **c** is a magnified image of the membrane particle highlighted in the upper-left image, and the lower image in **c** is a magnified image of the highlighted region in the upper-right image. Bars = 10 µm (**a**, left; **b**), 1 µm (**a**, right), 2 µm (**c**, left; **d**), and 200 nm (**c**, right). HEPES, 4-(2-hydroxyethyl)-1-piperazineethanesulfonic acid; SEM, scanning electron microscopy; TEM, transmission electron microscopy.

Live-CLEM

To obtain more detailed information on the formation of membrane particles, we analyzed cells treated with R12-Alexa488 using correlative light and electron microscopy after live-cell imaging (Live-CLEM) (**Figure 5** and **Supplementary Figure S8**).[21] This method, recently developed by Haraguchi and coworkers, is a powerful tool for monitoring TEM images of the same cells that were observed by time-lapse live imaging. We used it in an effort to confirm that the multilamellar vesicle structures described above were actually formed at the sites of peptide influx as a function of time. Live-cell imaging of HeLa cells treated with 5 µmol/l R12-Alexa488 was carried out at 37 °C using a confocal microscope. The cells were then fixed with GA 1 minute after membrane particles were observed (~2 minutes after addition of the peptide) (arrows in **Figure 5a** and **Supplementary Figure S8**). The fixed cells were then subjected to TEM, which revealed the formation of multilamellar membrane structures a short time after treatment of the cells with the peptide (**Figure 5**). Z-stack analysis of the TEM images revealed that the distribution of the multilamellar structures ranged from sections 1–10 (counting from the bottom to the top in 80-nm intervals) (**Figure 5d**). While the lower part of the particle (sections 1–6) was buried inside the cells, membrane structures extruding from the cell surface were also observed for the upper sections (7–10). Analysis of representative membrane particles suggested that their diameters and heights were in the ranges 0.5–1 µm and 2–3 µm, respectively. Similar membrane structures were also observed in cells treated with R12-Alexa488 at 4 °C (**Supplementary Figure S9**), suggesting that the structural alterations in plasma membranes were induced by an energy-independent, physicochemical interaction between R12-Alexa488 and the plasma membrane.

Importance of the attachment of hydrophobic moieties to the R12 peptide for membrane-particle formation

To assess the possible contribution of the fluorescent moiety to particle formation, we analyzed whether non-labeled R12 also triggered the formation of particle-like structures. Although particle structures were formed within 6 minutes after treatment with 5 µmol/l R12-Alexa488 (**Figure 6**), very few were observed after treatment with non-fluorescently labeled R12, even after treatment at a higher concentration (20 µnol/l) for several minutes (**Figure 6** and **Supplementary Figure S10a**). The application of non-labeled R12 at a concentration of 100 µmol/l yielded fewer particle-like structures within 8–10 minutes than treatment with 5 µmol/l R12-Alexa488 (**Supplementary Figure S10b**). These results suggest the potential contribution of the Alexa Fluor 488 moiety to particle formation. Considering the effect of Alexa Fluor 488 as a source of hydrophobicity, we next examined whether the attachment of other hydrophobic moieties also contributed to the ability of the peptide to induce particle formation. HAtag (YPYDVPDYA) is a short, relatively hydrophobic peptide that is used for protein and peptide detection via immunostaining and

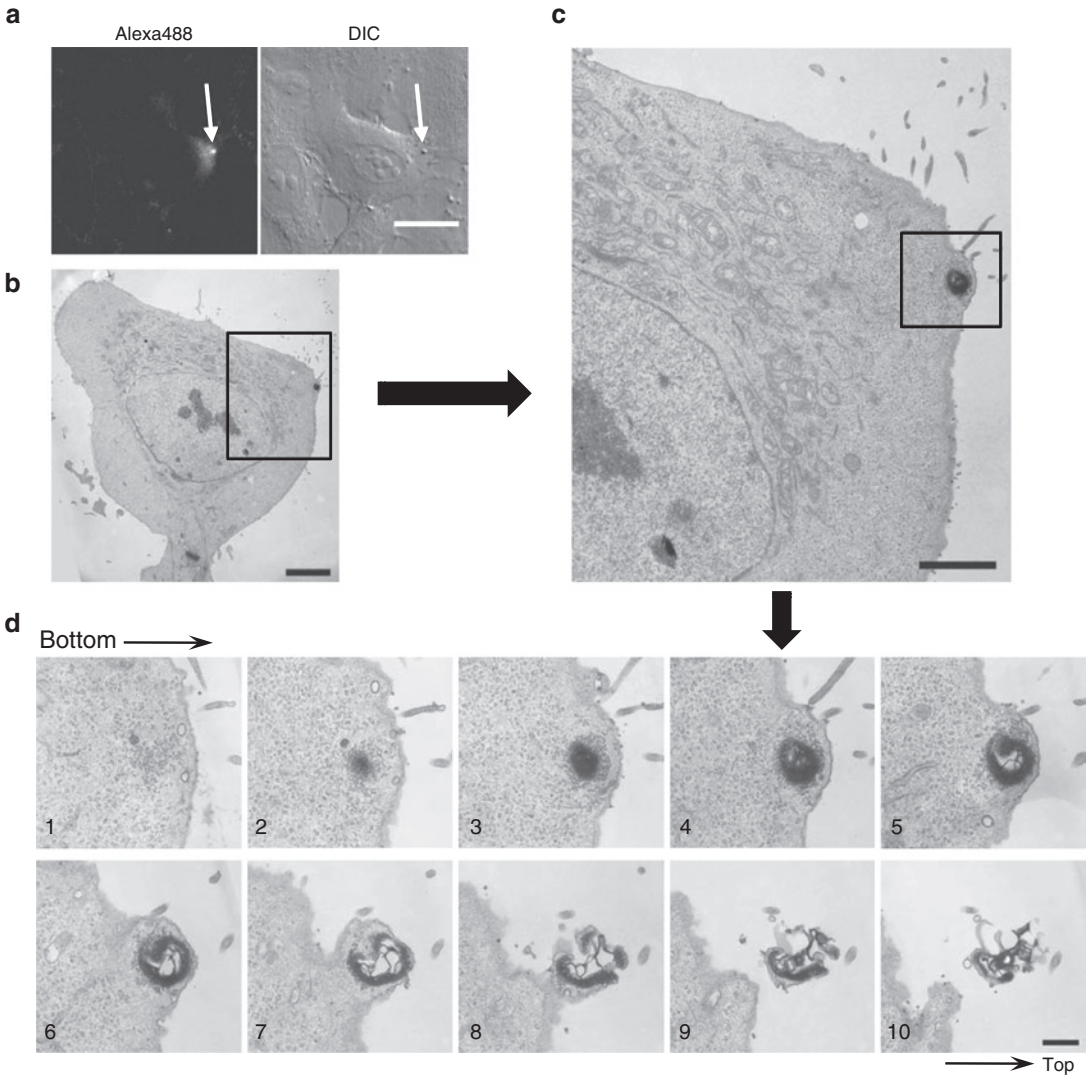

Figure 5 Correlative light and electron microscopy after live-cell imaging (Live-CLEM) of cells treated with R12-Alexa488. (**a**) HeLa cells were treated with R12-Alexa488 (5 µmol/l) in α-MEM(–) for 3 minutes (left, fluorescence image; right, DIC image). Bar = 20 µm. (**b**) Electron microscopic image of the cell identified with an arrow in **a**. Bar = 5 µm. (**c**) Enlarged image of the highlighted image in **b**. Bar = 2 µm. (**d**) Z-stack electron microscopic analysis of the highlighted area in **c**. Intervals = 80 nm. Bar = 500 nm. CLEM, correlative light and electron microscopy; DIC, differential interference contrast; MEM, minimum essential medium.

western blotting. We synthesized a hybrid peptide comprising R12 and HAtag sequences (R12-HAtag).

We next examined whether particles formed on the surfaces of HeLa cells following treatment with the R12-HAtag peptide. As expected, significant particle formation was observed following the treatment of cells with 20 µmol/l R12-HAtag (**Figure 6**). Particle formation accompanied direct peptide penetration through plasma membranes after treatment of HeLa cells with fluorescein-labeled R12 (R12-fluorescein) (**Supplementary Figure S10c**). In addition, we previously reported direct penetration of octa-arginine bearing a hexanoyl moiety on its N-terminus through plasma membranes,[22] which was also accompanied by membrane-particle formation (**Supplementary Figure S10d**). These results suggest that the attachment of an appropriate hydrophobic moiety to the R12 peptide or other arginine-rich peptides stimulates the formation of membrane particles on the cell surface, and this may have a strong correlation with the influx of peptide into cells.

Even modified with hydrophobic moieties, the R12 peptide seems unlikely to form aggregates or micelles in culture media. We examined the critical micelle concentration using R12-HAtag. Micelle/aggregate formation of the peptide should yield increases in the fluorescence intensity of the environment-sensitive fluorescence additive 1,6-diphenyl-1,3,5-hexatriene (DPH).[23] However, no significant increase in fluorescence intensity was observed, even after treatment with 6 mg/ml (*i.e.*, ~2 mmol/l) R12-HAtag (**Supplementary Figure S11**).

Assessment of plasma membrane integrity and involvement of membrane-repair mechanisms

Plasma membrane integrity upon membrane-particle formation was then confirmed by the lactate dehydrogenase-release assay, as reported previously.[16] The lack of significant leakage of lactate dehydrogenase from cells incubated with R12-HAtag for 30 minutes in phosphate-buffered saline (+) indicated integrity

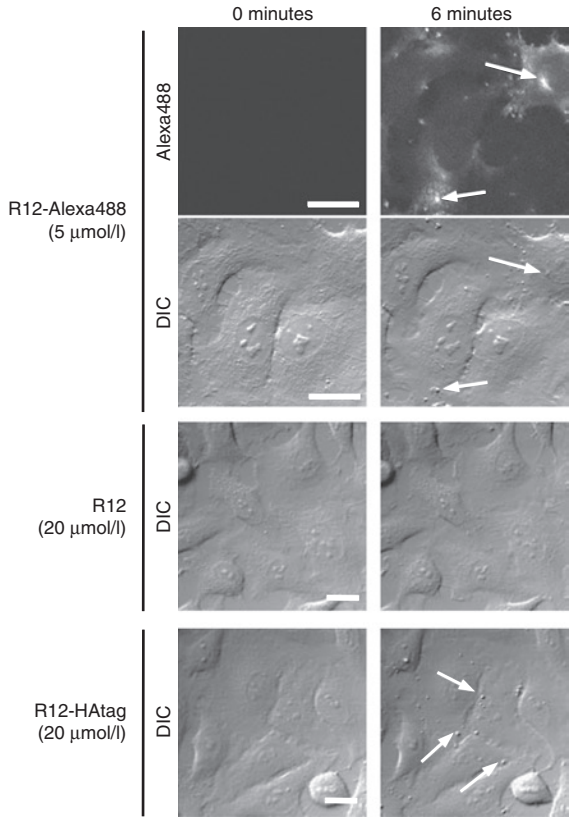

Figure 6 Importance of the hydrophobic moiety to the formation of particle structures. Time-lapse observation of HeLa cells incubated with R12-Alexa488 (5 μmol/l), R12 (20 μmol/l), or R12-HAtag (20 μmol/l). Time 0: images captured immediately before the addition of the arginine peptides. Arrows indicate membrane particles. Bar = 20 μm. DIC, differential interference contrast.

of the peptide-treated plasma membranes (**Supplementary Figure S12**).

Palm-Apergi *et al.* reported the induction of membrane-repair responses in cells treated with a model amphipathic peptide and penetratin.[24] These CPPs have basic and amphipathic structures. Thus, we examined whether the direct peptide influx through plasma membranes and membrane-particle formation were accompanied by a membrane-repair response. There are several membrane-repair systems, and one of the most studied of these mechanisms is mediated by exocytosis of lysosomes or endosomes.[25] If the lysosome-mediated membrane-repair response is induced at the location of membrane-particle formation, lysosomal proteins should be exposed on the cell membranes, and the recruitment of lysosomal-associated membrane protein 2 (LAMP-2) to these regions should be observed.[24] However, LAMP-2 was not detected near these particles (**Supplementary Figure S13a**). We also examined the internalization of R12-Alexa488 in the presence of 10 mmol/l dithiothreitol (DTT). It has been reported that oxidative conditions are necessary for the membrane-repair machinery that uses MG53, and this membrane-repair system does not work in the presence of reducing agents such as DTT.[26] Membrane-particle formation accompanied R12-Alexa488 influx in the presence of DTT, suggesting that this oxidative repair system was not involved (**Supplementary Figure S13b**).

Further studies are required to determine the involvement of other membrane-repair systems to membrane-particle formation. However, our results indicate that the formation of membrane particles is not due to lysosome- or endosome-mediated membrane-repair responses.

Translocation of R12-Alexa488 into giant vesicles

To examine whether the formation of membrane particles can be solely explained by the interaction of membrane lipids with arginine-rich peptides, the influx of R12-Alexa488 was studied using giant vesicles (GVs) that mimic the composition of plasma membranes (27.5% 1,2-dioleoyl-*sn*-glycero-3-phosphocholine (DOPC), 12.2% 1,2-dioleoyl-*sn*-glycero-3-phospho-L-serine (DOPS), 17.0% 1,2-dioleoyl-*sn*-glycero-3-phosphoethanolamine (DOPE), 8.8% SM, and 34.5% cholesterol (Chol) (in mol%))[27] (**Supplementary Figure S14**). As membrane potential should play a crucial role in the translocation of the R12 peptide through membranes, liposomes were formed using a K^+-rich buffer (50 mmol/l K_2SO_4, 10 mmol/l Tris-HCl, and 200 mmol/l sucrose, pH 7.4) for the inside of the liposomes and a Na^+-rich buffer (50 mmol/l Na_2SO_4, 10 mmol/l Tris-HCl, and 200 mmol/l sucrose, pH 7.4) as the outside buffer, followed by the addition of valinomycin as a potassium-selective ionophore. These conditions led to translocation of potassium ions through the membranes to the outside of the GVs, with no permeation by sodium ions, yielding inside-negative membrane potentials. Although no significant translocation of R12-Alexa488 (2.5 μmol/l, peptide:lipid ratio = 1:10) was observed in the GVs in the absence of valinomycin treatment (**Supplementary Figure S14c**), influx of R12-Alexa488 was observed in ~30% of the valinomycin-treated GVs (**Supplementary Figure S14d**). Gramicidin A is a peptide ion channel that transports both potassium and sodium ions. Treatment of the GVs with gramicidin A yielded no membrane potential and no peptide translocation (data not shown). These results highlighted the importance of membrane potential for the translocation of arginine-rich peptide through membranes.

Particle-like lipid domains that accumulated peptide were observed on the liposomal membrane (arrows in **Supplementary Figure S14c,d**). However, similar structures were also found on the liposomes before treatment with R12-Alexa488 (arrow in **Supplementary Figure S14a**), suggesting that these lipid structures were not formed by interaction with R12-Alexa488. It is possible that the penetration of peptide into living cells occurs through peptide–lipid interactions in the presence of a membrane potential. However, other cellular components, including membrane proteins, sugar chains, or cytosolic proteins, would also be necessary for the formation of membrane particles.

Influx of R4-Alexa488 into cells treated with R12-HAtag

The influx of R12 peptides bearing hydrophobic moieties may lead to membrane particle formation. This may be accompanied by local and transient alterations in the lipid bilayer structure. Coincubation with an R12 peptide bearing a hydrophobic moiety may also promote the translocation of peptides with low membrane permeability. To examine this hypothesis, R4-Alexa488 was employed as a model molecule with limited membrane permeability.[6]

HeLa cells were treated with R4-Alexa488 (10 μmol/l) in the presence of non-labeled R4-, R12-, and R12-HAtag peptides. As expected, a marked increase in the cellular uptake of R4-Alexa488 was observed in the presence of 20 μmol/l R12-HAtag (**Figure 7a**, rightmost column). Efficient influx of R4-Alexa488 and membrane-particle formation were also observed by confocal microscopy (**Figure 7b**, bottom right panels). In contrast, only a slight increase in the cellular uptake of R4-Alexa488 (10 μmol/l) was observed in cells that were cotreated with non-labeled R12 (20 or 100 μmol/l) (**Figure 7a**, middle column), even though confocal microscopic observation showed diffuse signals for R4-Alexa488 (**Figure 7b**, upper-right panels). Addition of non-labeled R4 (60 μmol/l) did not significantly increase the cellular uptake of R4-Alexa488.

Note that when GC-Alexa488, which contains no arginine residues, was applied at a concentration of 10 μmol/l in the presence of 20 μmol/l R12-HAtag, a significant influx of GC-Alexa488 into cells occurred, although the influx was weaker than that observed with R4-Alexa488 (**Figure 7c**, right).

The above results suggest that (i) R12 peptides bearing hydrophobic moieties have a much greater ability to directly penetrate into cells through the plasma membrane; (ii) membrane-particle formation may accompany the influx of peptides into cells; and (iii) the influx of R12-HAtag may lead to transient structural alterations in membrane lipid bilayers that allow the translocation of R4-Alexa488 and GC-Alexa488, which are otherwise unable to permeate the plasma membrane.

DISCUSSION

The careful live-cell observations performed in this study clearly revealed that direct internalization of R12-Alexa488 is accompanied by several events, including the formation of concentrated peptide regions and membrane particles, together with membrane inversion and the accumulation of negatively charged membrane components in the vicinity of the influx sites. In addition, electron microscopic analysis revealed the detailed structures of the membrane particles, which consisted of small vesicles stacked on top of each other. The interaction of R12-Alexa488 with the plasma membrane induced dynamic alterations in plasma membrane structures that led to the direct influx of the peptide. In addition, we showed that the conjugation of R12 to Alexa Fluor 488 or HAtag was important for the formation of the particles, which strongly suggests that the hydrophobic properties of the conjugated moiety may be important for accelerating R12 peptide-dependent penetration into the cell. The addition of hydrophobic moieties to the R12 peptide may increase its amphiphilicity or detergent-like activity. However, considering that the direct internalization of these peptides is not accompanied by apparent membrane impairment, the mechanisms of translocation of R12 conjugated

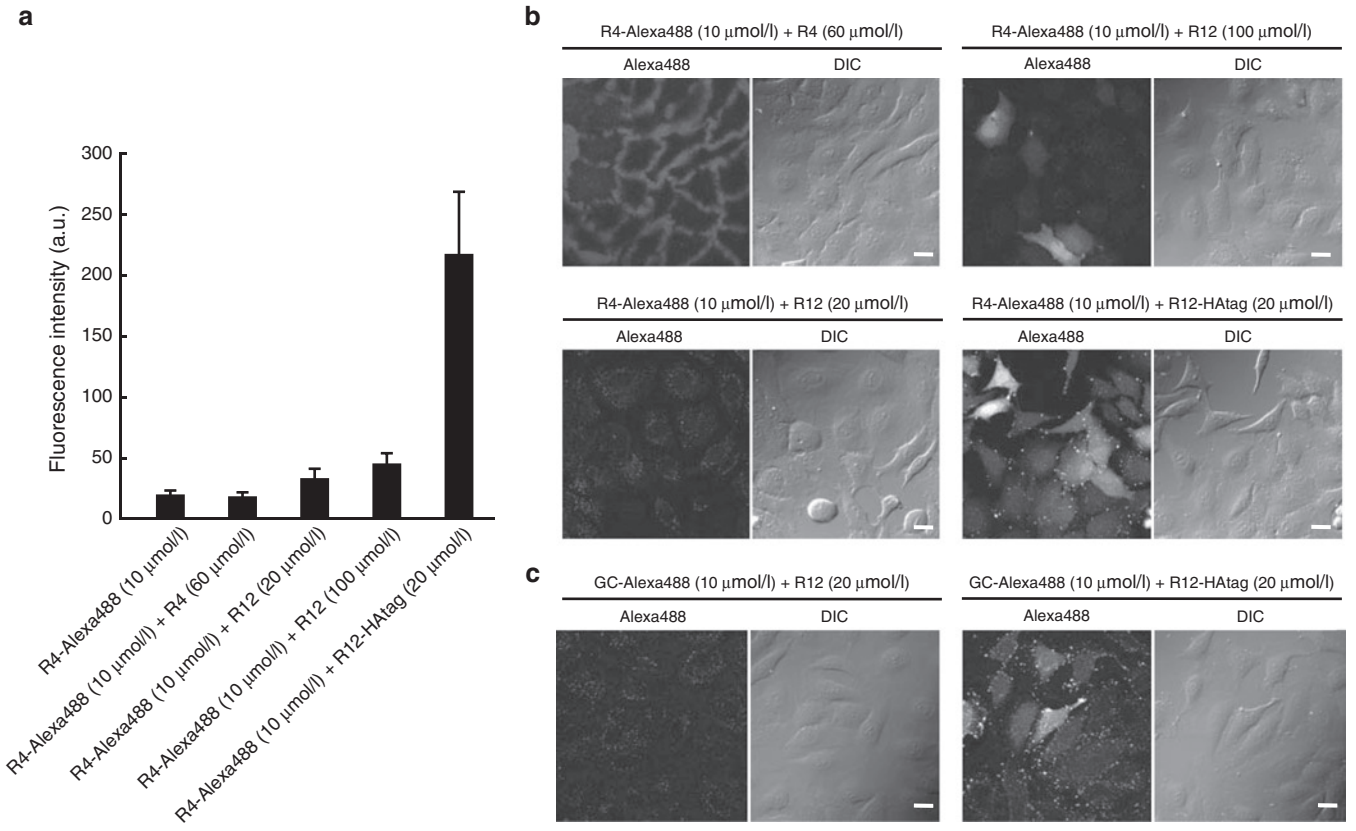

Figure 7 Coincubation with R12-HAtag stimulated the internalization of R4-Alexa488. (**a**) FACS analysis of the cellular uptake of R4-Alexa488 (10 μmol/l) in the presence or absence of R4 (60 μmol/l), R12 (20 μmol/l or 100 μmol/l), or R12-HAtag (20 μmol/l). Treatment at 37 °C for 10 minutes. Data show the mean ± SD (n = 3). (**b**) Confocal microscopic analysis of the cellular uptake of R4-Alexa488 in the presence of R4 (60 μmol/l), R12 (20 μmol/l or 100 μmol/l), or R12-HAtag (20 μmol/l). (**c**) Confocal microscopic analysis of the cellular uptake of GC-Alexa488 in the presence of R12 (20 μmol/l) or R12-HAtag (20 μmol/l). Bar = 20 μm. a.u., arbitrary unit; DIC, differential interference contrast; FACS, fluorescence-activated cell sorting.

to Alexa Fluor 488 or HAtag cannot be explained by simple membrane perturbation or transient pore formation, as was observed for cationic amphiphilic antimicrobial peptides.[28]

We and others have previously reported the direct flux of oligoarginine peptides through specific points on the plasma membrane in the absence of serum or at relatively high peptide concentrations.[14,16] However, the formation of unique particle structures associated with the sites of peptide influx is novel to this study. Note that the particles do not possess the simple bleb-like structure of outwardly expanding plasma membranes,[29] but have a complex yet unique structure formed from multiple vesicles with multilamellar membranes. Ziegler *et al.* reported the formation of dense aggregates on the surfaces of fibroblast cells treated with the Tat peptide.[30] However, the aggregates were different in size and shape from the particles observed in this study.

Although the mechanism by which these particle-like structures are formed remains unclear at present, cellular components other than lipids are likely involved in morphological alterations of the plasma membrane and consequent peptide influx into the cytosol. Membrane-associated negatively charged molecules such as sialic acids may also be directly or indirectly involved in this process because those molecules can form complexes with oligoarginine peptides through electrostatic interactions. The absence of obvious particle-like structures after addition of R12 to GVs further supported our assumption that membrane-particle formation in living cells is not due to the simple interaction of the peptides with lipids. Obviously, further analysis is required to identify the cellular components responsible for interactions with, and structural alterations of, the plasma membrane.

The formation of the membrane particles may be highly dependent on the number of arginine residues in the peptide. The R12 peptide has a stronger affinity for the plasma membrane than the R8 and R4 peptides and more strongly induces direct influx. Conjugation of a hydrophobic segment to the R12 peptide may further increase the interaction of the peptide to the plasma membrane and thereby induce direct influx of the peptide and the formation of the unique particle-like membrane structures. The formation of multilamellar membrane structures strongly suggests the involvement of membrane fusion or hemifusion in this process. Increasing the amphiphilicity of the R12 peptides through the attachment of a hydrophobic segment and the potential ability of arginine-rich CPPs to induce curvature in the membrane[31–34] may also play roles in the formation of the unique membrane structures.

Strong fluorescent signals of Alexa-labeled R12 peptide observed inside the membrane particles suggested the entrapment of the R12 peptide in the multilamellar structure. It is unclear whether the peptide penetrated through the multilamellar structures to enter the cells. However, the peptides likely form complexes with other membrane-associated molecules in the particles, and it would be inefficient to translocate through multiple membranes while dissociating from these molecules. Alternatively, peptide influx into cells may lead to local perturbation of the membrane structures to yield particle-like structures. Peptide influx may also lead to phase separation of the membranes by the recruitment of GM1 and SM to the sites of peptide internalization, as observed in this study. Consistent with this, the direct penetration of nonaarginine (R9) was recently reported to induce the translocation of acid SMase to the outer leaflet of the plasma membrane and, subsequently, ceramide formation.[35] The induction of phase separation upon particle formation may accelerate the influx of peptides into cells through the membranes.[36]

The results obtained in this study provide novel insights from the perspective of drug delivery. First, the attachment of Alexa Fluor 488 or HAtag significantly enhanced membrane-particle formation. This should shed light on ways of optimizing R12 as an intracellular delivery vector because direct penetration of R12 can be accelerated by the attachment of hydrophobic cargo compounds of relatively low molecular weights. Second, with the help of R12-HAtag, molecules with low membrane permeability (R4-Alexa488 and GC-Alexa488) were successfully delivered to the cytosol. The dynamic structural alterations in the plasma membrane induced by R12-HAtag may allow synchronized translocation of these molecules into cells, while the affinity of the conjugate for the cell surface may be an important factor determining the efficacy of translocation.

In summary, through the above studies on the mechanisms of direct internalization of the R12 peptide, we have identified novel properties of oligoarginine peptides that induce unique multimeric particle formation. The above results should have an impact on the design of novel intracellular delivery systems for low-molecular-weight compounds that cannot permeate the cell membrane.

MATERIALS AND METHODS

Peptides. All the peptides used in this study were chemically synthesized and fluorescently labeled using Alexa 488 or Alexa568 C_5 maleimide sodium salt (Invitrogen, Carlsbad, CA) or 5-(Iodoacetamido)fluorescein (Sigma, St Louis, MO) as already reported.[13] The actual sequences of the synthesized peptides are as follows: R12, NH_2-$(Arg)_{12}$-amide; R12-Alexa488, NH_2-$(Arg)_{12}$-Gly-Cys(Alexa488)-amide; R12-HAtag, NH_2-$(Arg)_{12}$-$(Gly)_2$-Tyr-Pro-Tyr-Asp-Val-Pro-Asp-Tyr-Ala-amide; R4, NH_2-$(Arg)_4$-amide; R4-Alexa488, NH_2-$(Arg)_4$-Gly-Cys(Alexa488)-amide; GC-Alexa488, NH_2-Gly-Cys(Alexa488)-amide; R12-fluorescein, NH_2-$(Arg)_{12}$-Gly-Cys(fluorescein)-amide; R12-Alexa568, NH_2-$(Arg)_{12}$-Gly-Cys(Alexa568)-amide; Hexanoyl R8-Alexa, $C_5H_{11}CO$-$(Arg)_8$-Gly-Cys(Alexa488)-amide.

Correlative light and electron microscopy after live-cell imaging (Live-CLEM). HeLa cells were cultured on a grid-based, glass-bottomed culture dish (Iwaki, Chiba, Japan). The cells were washed with α-minimum essential medium (MEM)(–) twice, incubated with 150 µl of α-MEM(–), and allowed to settle for 10 minutes in an MI-IBC microchamber attached to the stage of an inverted microscope. The incubator provided a humidified atmosphere containing 5% CO_2 and a temperature of 37 °C. Next, R12-Alexa488 (final concentration, 5 µmol/l) was added to the cells and time-lapse imaging was carried out. Glutaraldehyde (final concentration 2.5%) was added to the medium at the desired time point (1, 2, or 5 minutes) after membrane particles were observed, and the cells were allowed to settle before fixation. After washing three times with phosphate-buffered saline, three-dimensional images of the same cells (at 0.2-µm intervals) were acquired using a confocal microscope equipped with a 60× objective lens (oil, NA 1.35).

TEM analysis of the same cells observed by confocal microscopy was conducted as described previously.[21] Briefly, cells were postfixed with 1% OsO_4 (cat. no. 3002; Nisshin EM, Tokyo, Japan). After partial dehydration through incubation in 30% ethanol for 1 minute, 50% ethanol for 3 minutes, and 70% ethanol for 5 minutes, the cells were stained with 2% uranyl acetate (cat. no. 554-85072; Wako Pure Chemical Industries, Osaka, Japan) in 70% ethanol for 30 minutes, and then completely dehydrated through incubation in 90% ethanol for 5 minutes and 100% ethanol for 5 minutes. The cells were then embedded in epoxy resin through incubation with 10, 30, 50, 70, and 90% (vol/vol) Epon812 (cat. no. T024; TAAB

Laboratories Equipment, Berkshire, UK) in ethanol and 100% Epon812. The epoxy block containing the same cells that had been observed by confocal microscopy was trimmed according to the grid address on the glass base, and sectioned using an ultramicrotome (Leica Microsystems, Wetzlar, Germany), yielding ultrathin sections with a thickness of 80 nm. These sections were stained with 4% uranyl acetate for 15 minutes and a commercial ready-to-use solution of lead citrate (cat. no. 18-0875-2; Sigma) for 1 minute. Images were acquired using a JEM-2000EX electron microscope (80 kV; JEOL, Tokyo, Japan).

Details of the other experiments performed are provided in the **Supplementary Materials and Methods**.

SUPPLEMENTARY MATERIAL

Figure S1. Direct internalization of R12-Alexa488 into the cytosol, initiated at a site on the plasma membrane with an intense fluorescent signal.

Figure S2. The R12-Alexa488 spots strongly colocalize with transiently formed membrane particles.

Figure S3. Time-lapse images of cells incubated with R12-Alexa488 at 15°C and R4-Alexa488 at 37°C.

Figure S4. The effect of macropinocytosis inhibitors on the formation of membrane particles.

Figure S5. Effect of membrane potential on particle formation and influx of R12-Alexa488 into cells.

Figure S6. Immunofluorescence staining of MβCD-treated and control cells with lysenin.

Figure S7. Effects of fixation procedures on the internalization of R12-Alexa488 and cellular morphology.

Figure S8. Live-cell imaging for correlative light and electron microscopy (CLEM) (see also Figure 5).

Figure S9. Correlative light and electron microscopy (CLEM) of cells treated with R12-Alexa488 for 1 minute at 4 °C.

Figure S10. Treatment of HeLa cells with nonlabeled R12, R12-fluorescein, and Hexanoyl R8-Alexa488.

Figure S11. Analysis of critical micelle concentration (CMC).

Figure S12. Assessment of plasma membrane integrity by LDH release assay.

Figure S13. Examination of plasma membrane-repair responses.

Figure S14. R12-Alexa488 translocation into GVs that mimic plasma membranes with membrane potential.

Video S1. Time-lapse images of the cells incubated with R12-Alexa488 (5 µmol/l) that correspond to Figure S1.

Materials and Methods

ACKNOWLEDGMENTS

This work was supported in part by Grants-in-Aid for Scientific Research from the Ministry of Education, Culture, Sports, Science and Technology of Japan to I.N., S.K., T.H., and S.F. T.T. and H.H. are grateful for a JSPS Research Fellowship for Young Scientists and S.P. is grateful for a JSPS Postdoctoral Fellowship for Foreign Researchers. The authors are grateful to Takamasa Hanaichi for his technical assistant with the electron microscopic observations for Figure 4. The authors declared no conflict of interest.

REFERENCES

1. Joliot, A and Prochiantz, A (2004). Transduction peptides: from technology to physiology. *Nat Cell Biol* **6**: 189–196.
2. Futaki, S (2008). Membrane permeable peptide vectors: chemistry and functional design for the therapeutic applications. *Adv Drug Deliv Rev* **60**: 447.
3. Futaki, S, Suzuki, T, Ohashi, W, Yagami, T, Tanaka, S, Ueda, K *et al.* (2001). Arginine-rich peptides. An abundant source of membrane-permeable peptides having potential as carriers for intracellular protein delivery. *J Biol Chem* **276**: 5836–5840.
4. Rothbard, JB, Garlington, S, Lin, Q, Kirschberg, T, Kreider, E, McGrane, PL *et al.* (2000). Conjugation of arginine oligomers to cyclosporin A facilitates topical delivery and inhibition of inflammation. *Nat Med* **6**: 1253–1257.
5. Vivès, E, Brodin, P and Lebleu, B (1997). A truncated HIV-1 Tat protein basic domain rapidly translocates through the plasma membrane and accumulates in the cell nucleus. *J Biol Chem* **272**: 16010–16017.
6. Nakase, I, Takeuchi, T, Tanaka, G and Futaki, S (2008). Methodological and cellular aspects that govern the internalization mechanisms of arginine-rich cell-penetrating peptides. *Adv Drug Deliv Rev* **60**: 598–607.
7. Wender, PA, Galliher, WC, Goun, EA, Jones, LR and Pillow, TH (2008). The design of guanidinium-rich transporters and their internalization mechanisms. *Adv Drug Deliv Rev* **60**: 452–472.
8. Snyder, EL and Dowdy, SF (2005). Recent advances in the use of protein transduction domains for the delivery of peptides, proteins and nucleic acids in vivo. *Expert Opin Drug Deliv* **2**: 43–51.
9. Richard, JP, Melikov, K, Vives, E, Ramos, C, Verbeure, B, Gait, MJ *et al.* (2003). Cell-penetrating peptides. A reevaluation of the mechanism of cellular uptake. *J Biol Chem* **278**: 585–590.
10. Jones, AT (2007). Macropinocytosis: searching for an endocytic identity and role in the uptake of cell penetrating peptides. *J Cell Mol Med* **11**: 670–684.
11. Nakase, I, Niwa, M, Takeuchi, T, Sonomura, K, Kawabata, N, Koike, Y *et al.* (2004). Cellular uptake of arginine-rich peptides: roles for macropinocytosis and actin rearrangement. *Mol Ther* **10**: 1011–1022.
12. Wadia, JS, Stan, RV and Dowdy, SF (2004). Transducible TAT-HA fusogenic peptide enhances escape of TAT-fusion proteins after lipid raft macropinocytosis. *Nat Med* **10**: 310–315.
13. Nakase, I, Tadokoro, A, Kawabata, N, Takeuchi, T, Katoh, H, Hiramoto, K *et al.* (2007). Interaction of arginine-rich peptides with membrane-associated proteoglycans is crucial for induction of actin organization and macropinocytosis. *Biochemistry* **46**: 492–501.
14. Duchardt, F, Fotin-Mleczek, M, Schwarz, H, Fischer, R and Brock, R (2007). A comprehensive model for the cellular uptake of cationic cell-penetrating peptides. *Traffic* **8**: 848–866.
15. Fretz, MM, Penning, NA, Al-Taei, S, Futaki, S, Takeuchi, T, Nakase, I *et al.* (2007). Temperature-, concentration- and cholesterol-dependent translocation of L- and D-octa-arginine across the plasma and nuclear membrane of CD34+ leukaemia cells. *Biochem J* **403**: 335–342.
16. Kosuge, M, Takeuchi, T, Nakase, I, Jones, AT and Futaki, S (2008). Cellular internalization and distribution of arginine-rich peptides as a function of extracellular peptide concentration, serum, and plasma membrane associated proteoglycans. *Bioconjug Chem* **19**: 656–664.
17. Koivusalo, M, Welch, C, Hayashi, H, Scott, CC, Kim, M, Alexander, T *et al.* (2010). Amiloride inhibits macropinocytosis by lowering submembranous pH and preventing Rac1 and Cdc42 signaling. *J Cell Biol* **188**: 547–563.
18. Matsuzaki, K, Noguch, T, Wakabayashi, M, Ikeda, K, Okada, T, Ohashi, Y *et al.* (2007). Inhibitors of amyloid beta-protein aggregation mediated by GM1-containing raft-like membranes. *Biochim Biophys Acta* **1768**: 122–130.
19. Simons, K and Ikonen, E (1997). Functional rafts in cell membranes. *Nature* **387**: 569–572.
20. Yamaji, A, Sekizawa, Y, Emoto, K, Sakuraba, H, Inoue, K, Kobayashi, H *et al.* (1998). Lysenin, a novel sphingomyelin-specific binding protein. *J Biol Chem* **273**: 5300–5306.
21. Haraguchi, T, Kojidani, T, Koujin, T, Shimi, T, Osakada, H, Mori, C *et al.* (2008). Live cell imaging and electron microscopy reveal dynamic processes of BAF-directed nuclear envelope assembly. *J Cell Sci* **121**: 2540–2554.
22. Katayama, S, Hirose, H, Takayama, K, Nakase, I and Futaki, S (2011). Acylation of octaarginine: Implication to the use of intracellular delivery vectors. *J Control Release* **149**: 29–35.
23. Ryu, DW, Kim, HA, Song, H, Kim, S and Lee, M (2011). Amphiphilic peptides with arginines and valines for the delivery of plasmid DNA. *J Cell Biochem* **112**: 1458–1466.
24. Palm-Apergi, C, Lorents, A, Padari, K, Pooga, M and Hällbrink, M (2009). The membrane repair response masks membrane disturbances caused by cell-penetrating peptide uptake. *FASEB J* **23**: 214–223.
25. McNeil, PL and Steinhardt, RA (2003). Plasma membrane disruption: repair, prevention, adaptation. *Annu Rev Cell Dev Biol* **19**: 697–731.
26. Cai, C, Masumiya, H, Weisleder, N, Matsuda, N, Nishi, M, Hwang, M *et al.* (2009). MG53 nucleates assembly of cell membrane repair machinery. *Nat Cell Biol* **11**: 56–64.
27. D'Antuono, C, Fernández-Tomé, MC, Sterin-Speziale, N and Bernik, DL (2000). Lipid-protein interactions in rat renal subcellular membranes: a biophysical and biochemical study. *Arch Biochem Biophys* **382**: 39–47.
28. Matsuzaki, K, Nakamura, A, Murase, O, Sugishita, K, Fujii, N and Miyajima, K (1997). Modulation of magainin 2-lipid bilayer interactions by peptide charge. *Biochemistry* **36**: 2104–2111.
29. Tournaviti, S, Hannemann, S, Terjung, S, Kitzing, TM, Stegmayer, C, Ritzerfeld, J *et al.* (2007). SH4-domain-induced plasma membrane dynamization promotes bleb-associated cell motility. *J Cell Sci* **120**: 3820–3829.
30. Ziegler, A, Nervi, P, Dürrenberger, M and Seelig, J (2005). The cationic cell-penetrating peptide CPP(TAT) derived from the HIV-1 protein TAT is rapidly transported into living fibroblasts: optical, biophysical, and metabolic evidence. *Biochemistry* **44**: 138–148.
31. Lamazière, A, Wolf, C, Lambert, O, Chassaing, G, Trugnan, G and Ayala-Sanmartin, J (2008). The homeodomain derived peptide Penetratin induces curvature of fluid membrane domains. *PLoS ONE* **3**: e1938.
32. Afonin, S, Frey, A, Bayerl, S, Fischer, D, Wadhwani, P, Weinkauf, S *et al.* (2006). The cell-penetrating peptide TAT(48-60) induces a non-lamellar phase in DMPC membranes. *Chemphyschem* **7**: 2134–2142.
33. Mishra, A, Gordon, VD, Yang, L, Coridan, R and Wong, GC (2008). HIV TAT forms pores in membranes by inducing saddle-splay curvature: potential role of bidentate hydrogen bonding. *Angew Chem Int Ed Engl* **47**: 2986–2989.
34. Sakamoto, K, Takino, Y and Ogasawara, K. Methods for controlling membrane permeability of a membrane permeable substance and screening methods for a membrane permeable substance. In: USP appl 2005/0118204, 2 Jun 2005 (JP appl 2003-3774224, 4 Nov 2003).
35. Verdurmen, WP, Thanos, M, Ruttekolk, IR, Gulbins, E and Brock, R (2010). Cationic cell-penetrating peptides induce ceramide formation via acid sphingomyelinase: implications for uptake. *J Control Release* **147**: 171–179.
36. Montes, LR, Ruiz-Argüello, MB, Goñi, FM and Alonso, A (2002). Membrane restructuring via ceramide results in enhanced solute efflux. *J Biol Chem* **277**: 11788–11794.